

## Hard X-ray Lags in Cygnus X-1

D.J. Crary<sup>1</sup>, M.H. Finger<sup>1</sup>, C. Kouveliotou<sup>1</sup>, F. van der Hooft<sup>2</sup>,  
M. van der Klis<sup>2</sup>, W.H.G. Lewin<sup>3</sup> and J. van Paradijs<sup>2,4</sup>

### ABSTRACT

We have used the Fourier cross spectra of Cyg X-1, as obtained with BATSE during a period of almost 2000 days, to estimate the phase (or time) lags between X-ray flux variations in the 20–50 keV and the 50–100 keV bands as a function of Fourier frequency,  $\nu$ . We find that these lag spectra do not depend on source state, as measured by the fractional rms variations of the X-ray flux. For frequencies well below the Nyquist frequency the variations in the 50–100 keV band lag those in the 20–50 keV band by a time interval  $\tau \propto \nu^{-0.8}$ . Binning effects cause the observed hard X-ray time lags to decrease to zero at the Nyquist frequency. Some previous results on time lags were affected by these binning effects. At photon energies above 10 keV the time lags are approximately proportional to the logarithm of the ratio the energies of the passbands used.

*Subject headings:* X-rays: stars – stars: individual: Cyg X-1 – accretion, accretion disks

To appear in *Astrophysical Journal Letters*

### 1. Introduction

The delay of high-energy photons relative to low-energy photons in the X-ray brightness variations of Cygnus X-1 has been known for some time. The significance of these lags is their possible use as a diagnostic of the source of Compton upscattering of soft photons widely believed to be the origin of the hard spectral tail seen in Cyg X-1 and other black hole candidates (BHCs) (Miller 1995; Nowak & Vaughan 1996), as a probe of the dynamics of the Comptonization region itself (Miyamoto et al. 1988), and as a second-order statistic supplementary to the power spectrum in the determination of parameters in shot-noise models (Miyamoto et al. 1988).

---

<sup>1</sup>Universities Space Research Association, Huntsville, AL 35806.

<sup>2</sup>Astronomical Institute “Anton Pannekoek”, University of Amsterdam & Center for High-Energy Astrophysics, Kruislaan 403, NL-1098 SJ Amsterdam, The Netherlands.

<sup>3</sup>Massachusetts Institute of Technology, 37-627 Cambridge, MA, 02139.

<sup>4</sup>Department of Physics, University of Alabama in Huntsville, Huntsville, AL 35899.

The lags have been investigated using cross spectral analyses of the time variations of the source in different energy channels (van der Klis et al. 1995; see also Lewin, van Paradijs & van der Klis 1988). Miyamoto et al. (1988, 1989, 1992, 1993) have applied this technique to the BHCs Cyg X-1, GX 339–4, GS 2023+338, and GS 1124–338 with Ginga data, using various combinations of energy channels from 2–37 keV and a maximum sampling frequency of 125 Hz (Nyquist frequency,  $\nu_{\text{Nyq}} = 62.5$  Hz). Their results showed that the lag spectra of these BHCs (i.e., lags as a function of Fourier frequency) were very similar, severally for the low state and the very high state which were covered in their observations. The amplitude of the lag in general increases with photon energy,  $E$ , except, perhaps, for  $E \lesssim 5$  keV. This consistent picture led Miyamoto et al. (1992) to refer to this lag properties as ‘canonical’ for BHC sources. The other type of X-ray binary for which the lag spectra have been well studied are the Z sources. These contain accreting neutron stars; they show different power spectral features, and have different lag properties (van der Klis et al. 1987).

In general, the results of Miyamoto et al. (1993) show a phase lag that increases as a function of frequency up to approximately  $\sim 5$  Hz, then decreases toward  $\nu_{\text{Nyq}}$ . At the highest frequencies, the uncertainties in the lag values become large enough to make the determination of any trend uncertain. The corresponding time lags decrease as the frequency increases towards  $\nu_{\text{Nyq}}$  where they are consistent with zero. At least in Cyg X-1, the phase lags depend on the average energies  $E_1$  and  $E_2$  of the energy bands used approximately as  $\ln(E_2/E_1)$  (Miyamoto et al. 1988).

We have used the approximately 2000 days of data from the Burst and Transient Source Experiment (BATSE) on the *Compton Gamma Ray Observatory* to investigate X-ray lags in variations from Cyg X-1, in a higher energy range than previously possible. Our data cover a large range in hard X-ray intensity and spectral slope (see Crary et al. 1996, and the X-ray light curves in Paciesas et al. 1997); our observations include time intervals in which an ultra-soft component is present; during these intervals Cyg X-1 was likely in the high or intermediate state (see Zhang et al. 1997; Belloni et al. 1996). A description of the data analysis is given in the next section. In sections 3 and 4 we compare our results to those of Miyamoto et al., and present our conclusions.

## 2. Observations

We calculated lags between the 20–50 and 50–100 keV energy bands of the  $\Delta T = 1.024$  s time resolution data obtained with the large-area detectors (LADs). Fast Fourier transforms were calculated in a way identical to that discussed in Crary et al. (1996a), with the addition of later observations. These transforms were created for 524.288 second intervals (512 time bins) in two energy channels, for all detectors with an angle of less than  $60^\circ$  to the direction of Cyg X-1 (from one to four detectors view the source during a particular pointing period). The average number of uninterrupted 512 bin segments available with the source unocculted by the Earth is approximately 40 per day. The complex cross amplitudes were created from the Fourier amplitudes  $a_j^i = \sum_k c_k^i \exp(i2\pi k j/n)$ , where  $n$  is the number of time bins,  $c_k^i$  is the detector count

rate in bin  $k = (0 \dots n - 1)$  and channel number  $i = (1, 2)$ , and  $j = (-n/2 \dots n/2)$  corresponds to Fourier frequencies  $2\pi j/n\Delta T$ . The cross spectra were normalized to the total detector count rates  $N_i$  in channel  $i$ , by analogy with the method of Leahy et al. 1983), and are given by  $C_j^{12} = \langle a_j^{2*} a_j^1 / \sqrt{N_1 N_2} \rangle$ , where the brackets refer to daily averaging. Errors on the averages of the real and imaginary parts of cross spectrum were calculated from their respective sample variances. For further averages of the cross spectrum these errors were propagated. The phase lag as a function of frequency is obtained from the cross spectrum as  $\phi_j = \arctan [\text{Im}(C_j^{12})/\text{Re}(C_j^{12})]$ . With the above definitions, lags in the hard X-ray variations appear as positive angles. For these data, deadtime induced cross-channel effects (van der Klis et al. 1987) will affect only the real part of the cross spectrum, reducing it by less than 5%.

### 3. Results

#### 3.1. Calculation of Phase and Time Lags

Because of the properties of the Fourier amplitudes (van der Klis 1989; Leahy et al. 1983) and the noise in the uncollimated BATSE detectors, the cross spectra for a large number of days must be averaged and converted to lag values to obtain sufficiently small errors. As shown by Crary et al. (1996a,b) the slope of the X-ray spectrum of Cyg X-1 and the amplitude of the variability are strongly correlated. This indicates also that within the low state the properties of Cyg X-1 are determined by a simple parameter, most likely the mass accretion rate. We have therefore used the squared fractional rms amplitude of the noise, integrated over the 0.03 – 0.488 Hz frequency range, as the relevant quantity with which to correlate the lag properties. Figure 1b-d shows the data grouped into three parts, i.e. those for which the daily averaged squared fractional rms values (between 0.03 and 0.488 Hz) are greater than 0.03 and less than 0.05, between 0.05 and 0.07, and greater than 0.07, respectively. The figure shows that to within the uncertainties, there is no obvious trend in the lag spectrum with source state. Figure 1a presents results obtained by averaging the cross spectra over the set of data with fractional rms squared values greater than 0.03.

These data show that at the lowest frequencies, the frequency dependence of the phase lag is consistent with zero phase lag; the phase lag rises to a peak value of 0.04 radians near 0.2 Hz and decreases above this point to a value to near zero radians at the  $\nu_{\text{Nyq}}$ . The resulting time lags,  $\tau_j = \phi_j/2\pi\nu_j$  (where  $\nu_j$  is the frequency in Hz of the  $j$ th frequency bin), are shown in Figure 2 (filled circles). These show a roughly power-law decrease above  $\sim 0.01$  Hz (exponent  $\sim -0.8$ ) with a break above 0.1 Hz, beyond which they decrease much more quickly.

The shape of the phase lag spectrum looks superficially like that found by Miyamoto et al. (1988) for Cyg X-1 and by Miyamoto et al. (1993) for GS 1124-68 and GX 339-4. For the case of Cyg X-1, however, the turn over in their phase lag spectrum occurred at  $\sim 30$  Hz, and these lags decreased to near zero at their Nyquist frequency (62.5 Hz). The similarity in the shape of

these spectra over the sampling time dependent frequency range suggests, by analogy with the finite-sampling effects in power spectral analyses (van der Klis 1989), that at least part of this shape (in particular the decrease toward the Nyquist frequency) is determined by binning and aliasing effects on the cross spectrum.

### 3.2. Systematic Effects

The effect of finite sampling on cross spectrum and lags can be calculated in a way similar to the analogous problem in the determination of power spectra (van der Klis 1989; see also Maejima et al. 1984).

The discrete form of the cross spectrum  $C_l^{12}$  for the pair of binned, continuous random functions  $x^j(t)$  with zero mean (with  $j$  equals 1 or 2) in terms of the cross spectrum  $\hat{C}^{12}$  of  $x^1(t)$  and  $x^2(t)$  is given by

$$C_l^{12} = \sum_{k=-\infty}^{\infty} \hat{C}^{12}\left(\frac{l}{n\Delta t} + \frac{k}{\Delta t}\right) \text{sinc}^2\left(\pi\left(\frac{l}{n} + k\right)\right)$$

where  $\text{sinc } x = \sin x/x$ ,  $n$  is the number of bins in a data segment,  $\Delta t$  is the bin width, and  $l = -n/2 \dots n/2$ . The sum over  $k$  represents the aliasing in the frequency domain due to the uniform sampling in the time domain (van der Klis 1989), and the  $\text{sinc}^2$  terms represent the effect of the averaging of the data over the finite time bin width.

To investigate the effect of binning on the phase and time lags, it is necessary to model the cross spectrum at frequencies above  $\nu_{\text{Nyq}}$ . Here we assume a cross spectrum of the form  $\hat{C}^{12}(\nu) = F(\nu)e^{i2\pi\nu\tau(|\nu|)}$ , where  $F(\nu)$ , the modulus of the cross spectrum, is independent of the detailed structure of the time lag  $\tau$  as a function of frequency, and the difference between the real and imaginary parts of the cross spectrum is determined by the complex exponential depending on  $\tau(|\nu|)$ . This phenomenological model has the simple interpretation that for  $\tau$  independent of  $\nu$  it represents a constant time lag. The real and imaginary parts of the cross spectrum are plotted in Figure 3. The shape of the real part of the cross spectrum is suggestive of the shape of a typical power spectrum, showing a ‘flat top’ at low frequency and a break at  $\sim 0.1$  Hz to a power law form at higher frequencies (Belloni & Hasinger 1991; Cray et al. 1996b). To test the validity of the simple model for the cross spectrum, we have modeled  $F(\nu)$  with a Lorentzian-type function  $F(\nu) = a_1/(1 + (|\nu|/a_2)^{a_3})$ , and assume that the time lag has a simple power-law form,  $\tau = \tau_0|\nu|^{-\alpha}$  from an inspection of the shape of the time lags in Figure 2 at a point well away from  $\nu_{\text{Nyq}}$ . These five parameters were then determined by a simultaneous fit of the real and imaginary parts of  $C_l^{12}$  to the cross spectral data. The best fit parameters are found to be  $a_1 = 1.5$ ,  $a_2 = 0.11$ ,  $a_3 = 1.3$  for  $F(\nu)$ , and  $\tau_0 = 0.0071$ ,  $\alpha = -0.78$  for  $\tau(|\nu|)$ .

Using the binning correction to this cross spectrum model, the fit to the data is shown as the dashed line in Figure 3. Without binning, the fit form is given by the dotted line in Figure 3. Because of the small values of  $\tau$  which are observed, the fit values are insensitive to the exact

functional form of  $\tau(|\nu|)$ , but the binning correction is a large effect. The effect of binning on the time lags calculated from this model is shown in Figure 2 (dashed line). We find that the time lag, away from  $\nu_{\text{Nyq}}$  depends on frequency,  $\nu$ , approximately as  $\nu^{-0.8}$  up to  $\nu \sim 0.2\text{Hz}$ . Above this frequency, the lags downturn, most of which is an artifact due to the data binning.

It should be stressed that these results are not meant to provide a definitive description of the cross spectra, but to illustrate the important effect of binning on the lag spectrum at frequencies above  $\sim 0.5\nu_{\text{Nyq}}$ . In this model, the calculation of the time lags is not sensitive to the detailed shape of  $F(\nu)$ , but it is clearly not adequately described by a simple Lorentzian-like function. Other potential systematic effects on the cross spectrum, such as ‘windowing’ in the time domain (van der Klis 1989), have not been considered. However, the implications of this simple model are clear. At least part of the decrease in the time lags with frequency observed by Miyamoto et al. (1992, 1993) must be attributed to binning effects. To obtain a precise determination of the phase or time lag as a function of frequency, these effects must be considered, or, since this effect dominates near the  $\nu_{\text{Nyq}}$  frequency, frequencies above  $\sim 0.5\nu_{\text{Nyq}}$  should be ignored.

Since we find that the lags are independent of rms fractional X-ray flux variations, we have combined our time lag results with those obtained by Miyamoto et al. (1989) for Cyg X-1. This allows us to study the photon energy dependence of the time lags over a much increased energy range. Miyamoto et al. (1989) found that the time lags between energy bands with average energies  $E_2$  and  $E_1$  are proportional to  $\epsilon = \ln(E_2/E_1)$ . For power law photon indices between  $-1.5$  and  $-2.5$  we find that for the BATSE energy bands  $\epsilon$  is in the range 0.802 and 0.833. To avoid the binning effects we have taken the time lag at  $\nu = 0.1$  Hz, for which we find  $\tau = 0.055 \pm 0.005$  s. Then the proportionality constant between time lag and the logarithm of the energy ratio  $\theta = \tau/\epsilon = 0.067 \pm 0.006$ . At the same frequency we infer from Figure 3 of Miyamoto et al. (1989) lags of 0.045 s, 0.030 s, and 0.088 s between the 1.2–4.7 keV and 4.7–9.3 keV bands, between the 4.7–9.3 keV and 9.3–14.0 keV bands, and between the 4.7–9.3 keV and 15.8–24.4 keV bands, respectively. The corresponding values of  $\theta$  are 0.045, 0.060 and 0.080, respectively (estimated accuracy  $\sim 10$  percent). This indicates that between the energy ranges below 10 keV and above 10 keV the ratio  $\theta$  of the time lags to  $\ln(E_2/E_1)$  increases; however, between  $\sim 10$  and 100 keV  $\theta$  does not change within the accuracy with which it has been determined.

#### 4. Conclusions

Based on our analysis of nearly 2000 days of BATSE data we have studied the time lags between the X-ray flux variations of Cyg X-1 in the 20–50 keV and 50–100 keV bands as a function of Fourier frequency. We find that the time lag spectra do not depend on source state as measured by the rms fractional variations of the X-ray flux. Over the range 0.01–0.2 Hz the hard lags  $\tau$  are proportional to  $\nu^{-0.8}$ . At frequencies above  $0.5\nu_{\text{Nyq}}$  the lags are artificially decreased (to zero at  $\nu_{\text{Nyq}}$ ) because of data binning. At least part of the ‘canonical’ time lag behavior of black holes, as defined by Miyamoto et al., is due to this binning effect. At photon energies above 10 keV

the time lags are approximately proportional to the logarithm of the ratio of the energies of the passbands used.

This project was performed within NASA grant NAG5-2560 and supported in part by the Netherlands Organization for Scientific Research (NWO) under grant PGS 78-277 and by the Netherlands Foundation for Research in Astronomy (ASTRON) under grant 781-76-017. Part of this work was completed while D.J.C held a National Research Council-NASA Research Associateship. F.v.d.H. acknowledges support by the Netherlands Foundation for Research in Astronomy with financial aid from NWO under contract number 782-376-011. W.H.G.L gratefully acknowledges support from the National Aeronautics and Space Administration, and J.v.P acknowledges support from NASA under contract NAG5-2755 and NAG5-3003.

## REFERENCES

- Belloni, T., & Hasinger, G. 1990, *A&A*, 227, L33
- Crary, D.J., et al. 1996, *ApJ*, 462, L71
- Crary, D.J., et al. 1996, *A&AS*, 120, 153
- Leahy, D. A., Darbro, W., Elsner, R. F., Weisskopf, M. C., Sutherland, P.G., Kahn, S., & Grindlay, J. E. 1983, *ApJ*, 226, 160
- Lewin, W.H.G., van Paradijs, J., and van der Klis, M. 1988, *Space Sci. Rev.*, 46, 273
- Maejima, Y., Makishima, M., Matsuoka, Y., Ogawara, Y., Oda, M., Tawara, Y., and Doi, K. 1984, *ApJ*, 285, 712
- Miller, M.C., 1995, *ApJ*, 441, 770
- Miyamoto, S., Kitamoto, S., Mitsuda, K., and Dotani, T. 1988, *Nature*, 336, 450
- Miyamoto, S, and Kitamoto, S. 1989, *Nature*, 342, 773
- Miyamoto, S., Kitamoto, S., Iga, S., Negoro, H, and Terada, K. 1992, *ApJ*, 391, L21
- Miyamoto, S., Iga, S., Kitamoto, S. Kamado, Y. 1993, *ApJ*, 403, L39
- Nowak, M.A., and Vaughan, B.A. 1996, *MNRAS*, 280, 227
- van der Klis, M., Hasinger, G., Stella, L. Langmeier, A., van Paradijs, J., and Lewin, W.H.G. 1987, *ApJ*, 319, L13
- van der Klis, M. 1989, in *Timing Neutron Stars*, ed. H. Ogelman & E.P.J. van den Heuvel, (Dordrecht: Kluwer Academic Publishers), 319
- Paciesas, W. S. et al., in *Proc. Forth Compton Symposium, Williamsburgs 1997*, in press.
- van der Klis, M. 1995, in *X-ray Binaries*, ed. W.H.G. Lewin, J. van Paradijs, & E.P.J. van den Heuvel (London: Cambridge University Press), 252

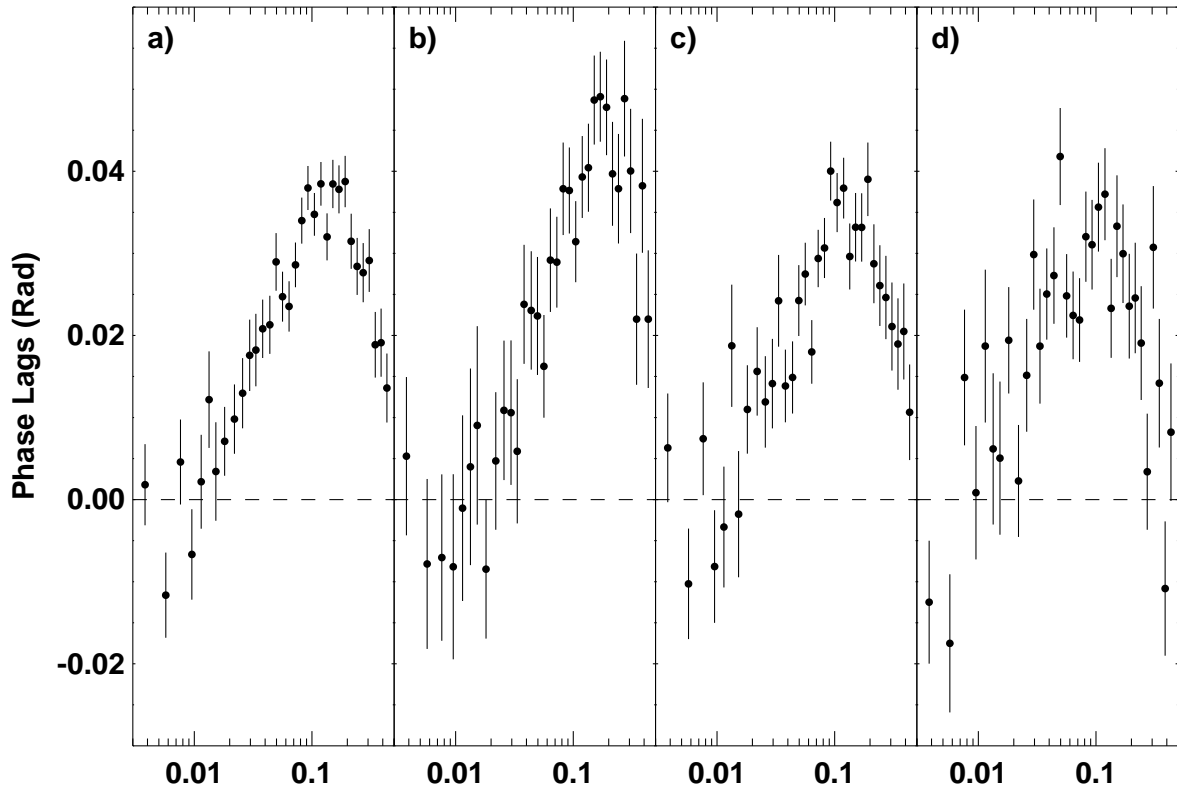


Fig. 1.— Phase lags between 20-50 keV and 50-100 keV data for various daily averaged squared rms levels,  $s$ . a) All data with  $s > 0.03$ , b)  $0.03s < 0.05$ , c)  $0.05 < s < 0.07$ , d)  $0.07 < s$ .

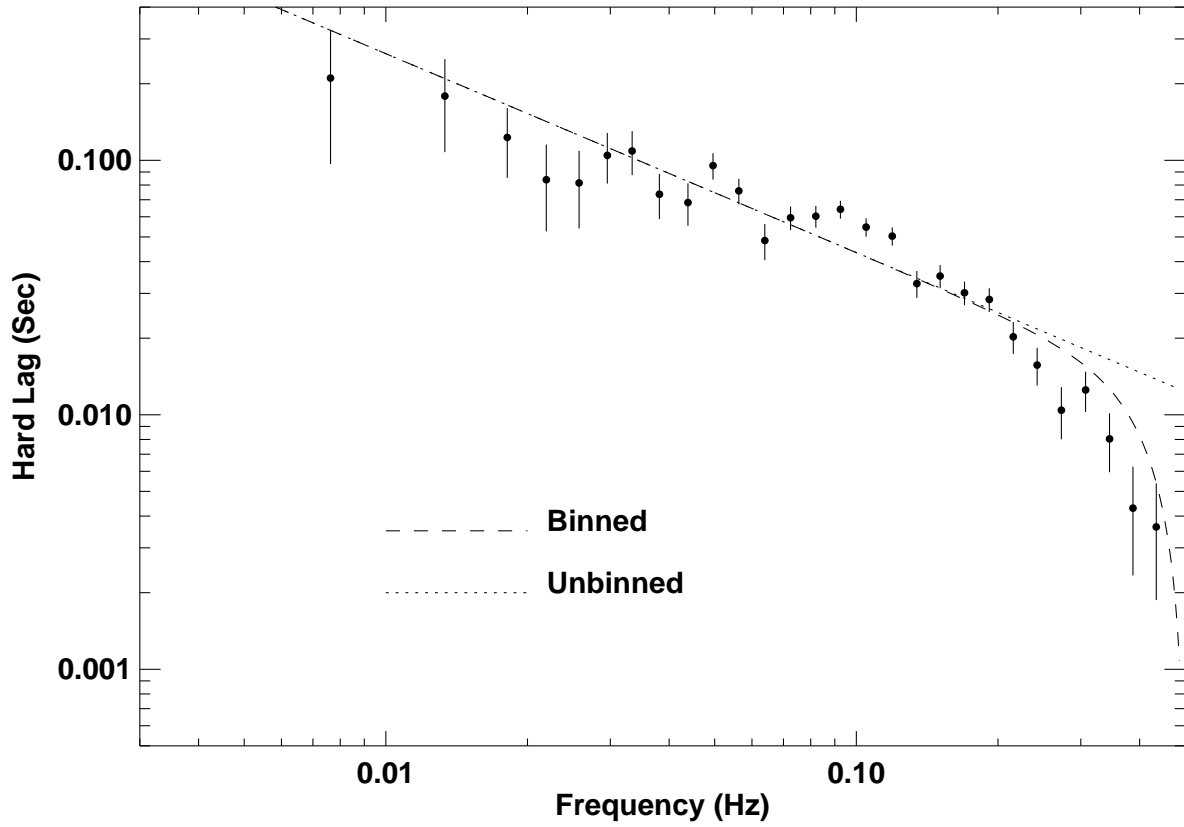


Fig. 2.— Time lags as a function of frequency. Solid circles denote values obtained by averaging over all data with fractional squared rms values greater than 0.03. The dashed line is the time lag obtained from a fit to the lag model including binning effects (see text). The dotted line is a power law with parameters determined from the model fit.

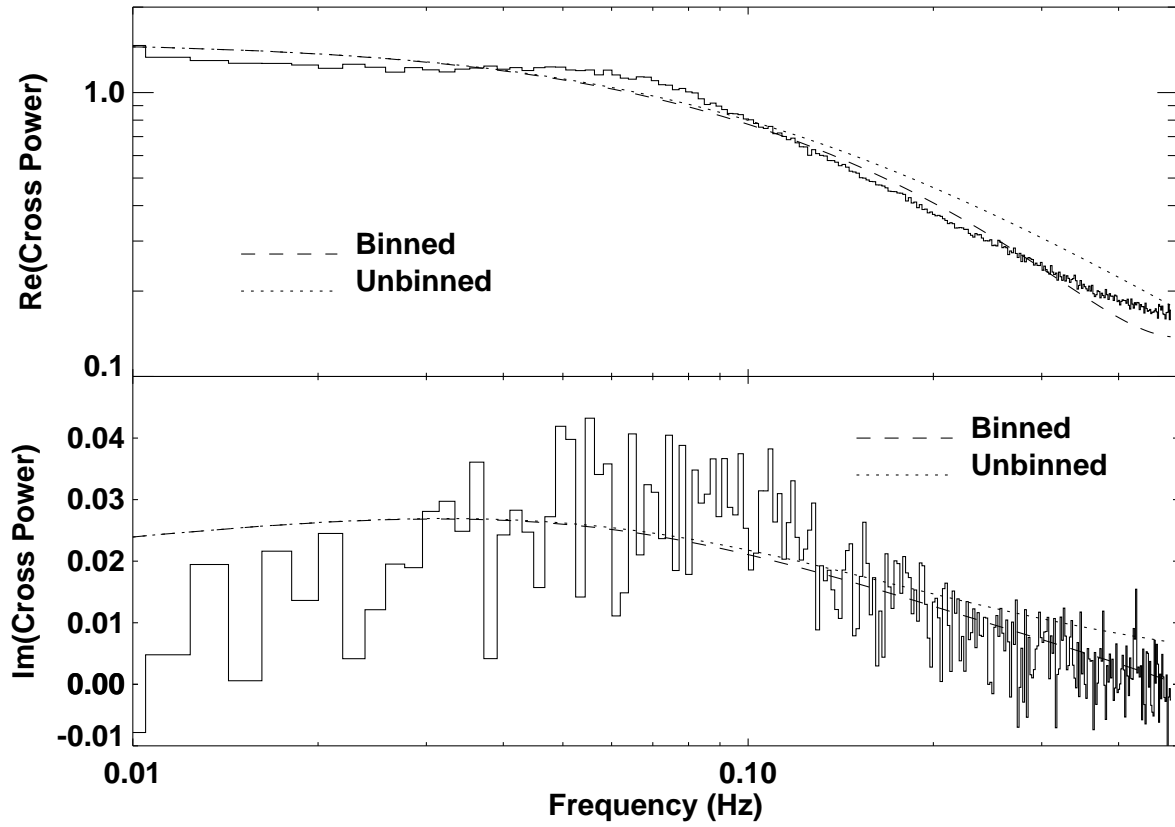


Fig. 3.— Real part (upper panel) and imaginary part of the cross spectrum. The dashed line is a fit of the lag model to the cross spectrum with the effects of binning included. The dotted line is the corresponding quantity without the effects of binning considered.